

# Homogenization of Layered Media: Intrinsic and Extrinsic Symmetry Breaking

Igor Tsukerman<sup>1</sup>, A N M Shahriyar Hossain<sup>1,2</sup>, Y. D. Chong<sup>3</sup>

<sup>1</sup>Department of Electrical and Computer Engineering, The University of Akron, OH 44325-3904, USA  
igor@uakron.edu

<sup>2</sup>Department of Electrical Engineering and Computer Science,  
Case Western Reserve University, Cleveland, OH, USA 44106

<sup>3</sup>School of Physical and Mathematical Sciences, Nanyang Technological University, 21 Nanyang Link, Singapore 637371  
yidong@ntu.edu.sg

A general homogenization procedure for periodic electromagnetic structures, when applied to layered media with asymmetric lattice cells, yields an effective tensor with magnetoelectric coupling. Accurate results for transmission and reflection are obtained even in cases where classical effective medium theory breaks down. Magnetoelectric coupling accounts for symmetry breaking in reflection and transmission when a non-symmetric structure is illuminated from two opposite sides.

A useful way to understand the properties of a periodic photonic heterostructure, such as a metamaterial or photonic crystal, is to represent it as a homogeneous effective medium. Effective medium descriptions are known to be accurate in the long-wavelength limit  $a/\lambda \rightarrow 0$ , where  $a$  is the unit cell size and  $\lambda = 2\pi c/\omega$  is the free-space wavelength, but break down when  $a/\lambda$  becomes appreciable [1–6]. A qualitative manifestation of this breakdown occurs when there are *incompatible symmetries* between the scattering characteristics of the original heterostructure and the respective homogenized sample.

As an example, consider wave propagation in a dielectric multilayer consisting of repeated layers labeled  $\alpha$  and  $\beta$ , surrounded by air, as shown in Fig. 1(a). The layers have unequal dielectric constants  $\epsilon_\alpha$  and  $\epsilon_\beta$  (which may be complex and dependent on the frequency  $\omega$ ), so that the heterostructure lacks mirror symmetry with respect to the normal direction  $n$ . In Fig. 1(b), the solid lines show the phases of the reflection coefficients  $\mathcal{R}_{\alpha\beta}$  and  $\mathcal{R}_{\beta\alpha}$ , calculated analytically using the transfer matrix technique [7], for  $s$ -polarized waves impinging normally on the structure with  $\alpha\beta\dots$  and  $\beta\alpha\dots$  layer orderings, respectively. (Reflection coefficients are the ratios of the complex amplitudes of the electric field in the reflected and incident waves.) In the static limit  $a/\lambda \rightarrow 0$ , the order of the layers is unimportant, but for larger values of  $a/\lambda$  the phases differ substantially [3–5, 8]. We call this effect, which arises from the lack of mirror asymmetry of the underlying heterostructure, *intrinsic symmetry breaking* (ISB) – to be contrasted with *extrinsic symmetry breaking* (p. 2).

At first glance, it seems that ISB cannot be faithfully reproduced by a homogenized slab, since a homogenous medium would have an inherent mirror symmetry ensuring that  $\mathcal{R}_{\alpha\beta} = \mathcal{R}_{\beta\alpha}$ . For instance, for  $s$ -waves and equal layer widths, standard quasi-static homogenization leads to a simple dielectric structure with the scalar effective permittivity  $\epsilon_{\text{eff}} = (\epsilon_\alpha + \epsilon_\beta)/2$ . The symmetry mismatch is also problematic for more sophisticated homogenization schemes; in particular, it cannot necessarily be resolved by *nonlocal* effective medium theories

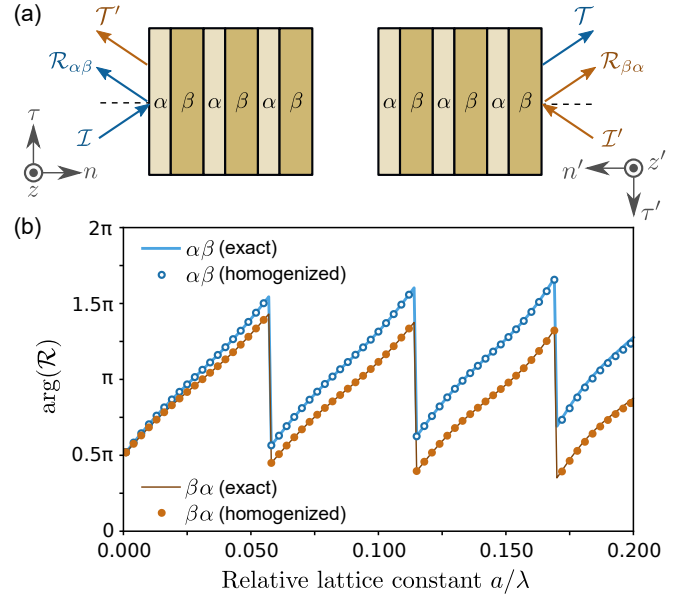


FIG. 1: (a) Schematic of a multilayer heterostructure consisting of two layers  $a$  and  $b$  repeated an integer number of times. The layers have dielectric constants  $\epsilon_\alpha$  and  $\epsilon_\beta$ , and are surrounded by air ( $\epsilon = 1$ ). (b) Phases of the two reflection coefficients  $\mathcal{R}_{\alpha\beta}$  and  $\mathcal{R}_{\beta\alpha}$  versus relative lattice constant  $a/\lambda$ , where  $\lambda$  is the free space wavelength. The multilayer has  $\epsilon_\alpha = 1$ ,  $\epsilon_\beta = 5$ , equal layer widths  $d_\alpha = d_\beta = a/2$ , with a total of 5 lattice periods (10 layers). The incident plane waves are  $s$  polarized (i.e.,  $\mathbf{E}$  parallel to  $z$  and  $\mathbf{H}$  lying in the  $n$ - $\tau$  plane). Solid lines: exact values calculated via the transfer matrix technique; markers: results for the the homogenization method described in the text.

[1, 2, 6, 9], whereby effective material parameters depend on the Fourier-space wavevector  $\mathbf{k}$ . (In real space, this results in non-pointwise relations between the fields.) To account for ISB, Lei *et al.* introduced an artificial matched layer on the illumination side [8]; however, this is not satisfactory, since an effective medium ought to reflect the intrinsic characteristics of the structure, independent of the illumination conditions.

Here, we show that an appropriate *local* homogenization scheme can accurately account for ISB via magneto-electric (ME) couplings in the effective material tensor. Artificial matching layers [8] or more complicated non-local formulations are not required. Details about the homogenization scheme are given below; when applied to the above multilayer structure, it produces the values plotted as markers in Fig. 1(b), which are in excellent agreement with the exact transfer matrix results. In particular,  $\arg(\mathcal{R}_{\alpha\beta}) = \arg(\mathcal{R}_{\beta\alpha})$  in the  $a/\lambda \rightarrow 0$ , but these values differ for larger values of  $a/\lambda$ , so that ISB is quantitatively accounted for.

A related but different effect arises when the external media on the two sides of the structure are different. In that case, not only the phases but also the magnitudes of the reflection coefficients may differ [3]. We refer to this as *extrinsic symmetry breaking* (ESB). When the medium on one side is optically denser than the static average in the slab, different layer orderings can produce extremely different reflection coefficients when the incident wave is close to the critical angle for total internal reflection (the phenomenon does not contradict optical reciprocity [10]). As we shall see, the effects of ESB can also be successfully accounted for by homogenization with ME coupling.

To understand the origin of ME coupling, we first consider the simple case of a lossless homogeneous medium with two *s*-polarized plane waves propagating in opposite axial directions  $\pm n$ , indicated in Fig. 1(a). The respective equal-magnitude wave vectors are  $\pm \mathbf{q} = \pm k_0 \hat{\mathbf{q}}$ , where  $\hat{\mathbf{q}}$  is a unit vector, and the respective electric and magnetic field components are

$$E_z^\pm = E_0^\pm \exp(\pm i k_0 \hat{\mathbf{q}} \cdot \mathbf{r}), \quad H_\tau^\pm = H_0^\pm \exp(\pm i k_0 \hat{\mathbf{q}} \cdot \mathbf{r}), \quad (1)$$

where  $\mathbf{r} = (n, \tau, z)$ . The waves satisfy Maxwell's equations  $\nabla \times \mathbf{E} = i k_0 \mathbf{B}$  and  $\nabla \times \mathbf{H} = -i k_0 \mathbf{D}$  under the  $\exp(-i\omega t)$  phasor convention. The medium is described by a material tensor  $\mathcal{M}$  whose matrix representation  $M$  in a given coordinate system satisfies

$$\Psi_{DB} = M \Psi_{EH}, \quad (2)$$

$$\Psi_{DB} = \begin{bmatrix} D_{0z}^+ & D_{0z}^- \\ B_{0\tau}^+ & B_{0\tau}^- \end{bmatrix}, \quad \Psi_{EH} = \begin{bmatrix} E_{0z}^+ & E_{0z}^- \\ H_{0\tau}^+ & H_{0\tau}^- \end{bmatrix}. \quad (3)$$

Normalizing the  $E_{0z}^\pm$  amplitudes to unity and applying Maxwell's equations gives

$$\Psi_{DB} = q_n \begin{bmatrix} -Y_+ & Y_- \\ -1 & 1 \end{bmatrix}, \quad \Psi_{EH} = \begin{bmatrix} 1 & 1 \\ Y_+ & Y_- \end{bmatrix}, \quad (4)$$

where  $Y_\pm = H_{0\tau}^\pm / E_{0z}^\pm$  are the wave admittances. Then

$$M = \Psi_{EH}^{-1} \Psi_{DB} = \frac{q_n}{Y_2 - Y_1} \begin{bmatrix} -2Y_1 Y_2 & Y_1 + Y_2 \\ -(Y_1 + Y_2) & 2 \end{bmatrix}. \quad (5)$$

The ME coupling is represented by the off-diagonal terms in  $M$ , and is absent if and only if  $Y_1 = -Y_2$ . This is the case for an ordinary homogeneous dielectric medium.

Note that this ME coupling is not equivalent to optical activity. It does not alter the polarization of the wave,

which remains *s*-polarized throughout. By contrast, the constitutive relations for optically active media typically include a contribution to  $\mathbf{D}$  in the direction of  $\mathbf{B}$ , as well as a contribution to  $\mathbf{B}$  in the direction of  $\mathbf{E}$  [11–13].

We now adopt the homogenization scheme described in Refs. 14, 15, which generates an effective tensor  $\mathcal{M}$  for a layered heterostructure by approximating the fields on two scales, one finer and the other one coarser than the lattice cell size. The fine-scale fields are approximated by basis sets of Bloch waves traveling in different directions. The coarse-scale fields consist of the respective generalized plane waves, which must satisfy (i) Maxwell's equations within the sample and (ii) Maxwell's boundary conditions for the tangential components of the electric and magnetic fields on the boundary of the sample. To satisfy (ii), the plane wave amplitudes  $\mathbf{E}_{0\alpha}$  and  $\mathbf{H}_{0\alpha}$  are computed as boundary averages of the periodic factors of Bloch waves; to satisfy (i), the  $M$  matrix is found by solving a linear algebra problem analogous to (2), except that now the  $\Psi_{DB}$  and  $\Psi_{EH}$  matrices are rectangular, with the number of columns equal to the number of basis functions. Hence (2) is in general interpreted in the least squares sense rather than as an exact equality [14, 15].

We apply this procedure to *s*-polarized waves in the multilayer heterostructure of Fig. 1(a) (the *p*-wave case can be dealt with similarly). To get an analytical insight, we take all the materials to be lossless, so that  $\epsilon_\alpha$  and  $\epsilon_\beta$  are real, and consider a fine-scale basis of only two Bloch waves, with their Bloch wave-numbers  $\pm q_n$  at the operating frequency:

$$e_1(n) = u(n) \exp(i q_n n) \quad (6)$$

$$h_{1\tau}(n) = -k_0^{-1} [q_n u(n) - i u'(n)] \exp(i q_n n) \quad (7)$$

$$e_2(n) = u^*(n) \exp(-i q_n n) \quad (8)$$

$$h_{2\tau}(n) = k_0^{-1} [q_n u^*(n) + i u'^*(n)] \exp(-i q_n n). \quad (9)$$

Here  $u(n)$  denotes the lattice-periodic factor for the electric field, and ‘\*’ indicates complex conjugates. On the coarse scale, our procedure defines the EH-amplitudes of plane waves as the *boundary values* ( $n = 0$ ) of the Bloch waves:

$$E_{0z}^+ = u(0), \quad H_{0\tau}^+ = -k_0^{-1} [q_n E_0^+ - i u'(0)], \quad (10)$$

$$E_{0z}^- = u^*(0), \quad H_{0\tau}^- = k_0^{-1} [q_n E_0^- + i u'^*(0)]. \quad (11)$$

The corresponding admittances are therefore

$$Y_1 = -k_0^{-1} [q_n - i \tilde{e}_1'(0) / \tilde{e}_1(0)] \quad (12)$$

$$Y_2 = k_0^{-1} [q_n + i \tilde{e}_1^{*'}(0) / \tilde{e}_1^*(0)]. \quad (13)$$

An explicit expression for the ME coupling term is

$$M_{12} = i \frac{q_n}{k_0} \frac{\text{Re } \eta}{\text{Im } \eta + q}, \quad \eta \equiv \frac{u'(0)}{u(0)}. \quad (14)$$

Hence the ME coupling arises from the difference in the boundary admittances of the Bloch waves. If the lattice cell possesses mirror symmetry, then derivative  $u'(0)$  vanishes, so  $M_{12} = 0$ .

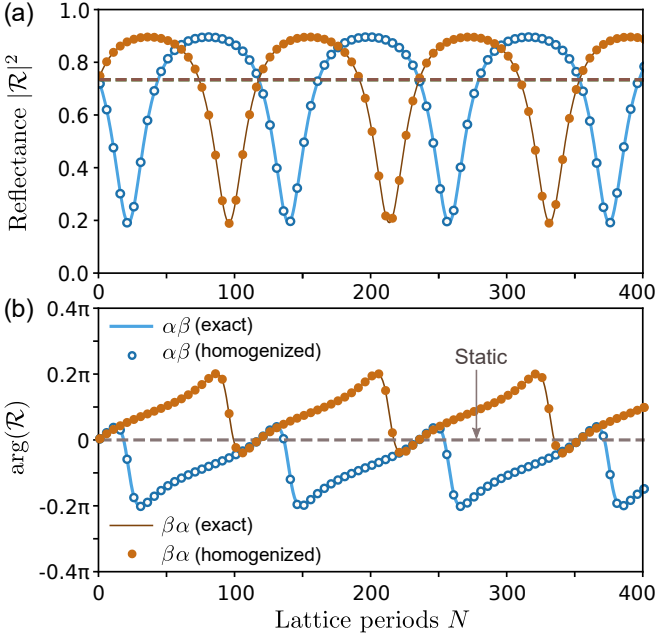


FIG. 2: Scattering characteristics of a multilayer with asymmetric external media. The structure consists of  $N$  identical cells, each containing two layers, ‘ $\alpha$ ’ and ‘ $\beta$ ’, with the thicknesses  $d_\alpha = d_\beta = 10$  nm and dielectric constants  $\epsilon_\alpha = 5$  and  $\epsilon_\beta = 1$ . Free-space wavelength  $\lambda = 500$  nm (i.e.  $a/\lambda = 0.04$ ). External dielectric constants are  $\epsilon_{\text{in}} = 4$  and  $\epsilon_{\text{out}} = 3$  on the sides of incidence and transmission, respectively. (These parameters match the ones of Ref. 3.) Incidence is at the critical angle (15). (a) reflectances  $|\mathcal{R}_{\alpha\beta}|^2$  and  $|\mathcal{R}_{\beta\alpha}|^2$ ; (b) reflection coefficient phases  $\arg(\mathcal{R}_{\alpha\beta})$  and  $\arg(\mathcal{R}_{\beta\alpha})$  vs.  $N$ . Solid curves: exact values calculated via the transfer matrix method. Markers: results for homogenization with magneto-electric coupling [14, 15]. Two layer orderings,  $\alpha\beta\dots$  and  $\beta\alpha\dots$ , exhibit significantly different behaviors. Static homogenization (horizontal dashed lines) yields qualitatively inaccurate results.

Importantly, the matrix representation of  $\mathcal{M}$  depends on the choice of coordinate system. If  $(n, \tau, z)$  is switched to the mirror-image system  $(n', \tau', z)$  shown in Fig. 1(a), the off-diagonal ME terms reverse sign. The effective medium is thus able to capture the effects of the broken mirror symmetry, as demonstrated by the numerical results of Fig. 1(b).

Turning now to ESB effects, we set the same parameters as in [3]: equal layer widths  $d_\alpha = d_\beta = a/2 = 10$  nm, dielectric constants  $\epsilon_\alpha = 5$  and  $\epsilon_\beta = 1$ , and free-space wavelength  $\lambda = 500$  nm. The effective permittivity for the  $s$  mode in the static limit ( $a/\lambda \rightarrow 0$ ) is  $\epsilon_{\text{stat}} = (\epsilon_\alpha d_\alpha + \epsilon_\beta d_\beta)/a = 3$ . The number of lattice cells  $N$  is allowed to vary. External dielectric permittivities are  $\epsilon_{\text{in}} = 4$  and  $\epsilon_{\text{out}} = 3$  on the sides of incidence and transmission, respectively. These parameters match the ones of Ref. 3 and, since  $\epsilon_{\text{in}} \neq \epsilon_{\text{out}}$ , give rise to ESB. In the static limit, the critical angle for total internal reflection is

$$\theta_{\text{crit}} = \sin^{-1} \sqrt{\epsilon_{\text{stat}}/\epsilon_{\text{in}}} = 60^\circ. \quad (15)$$

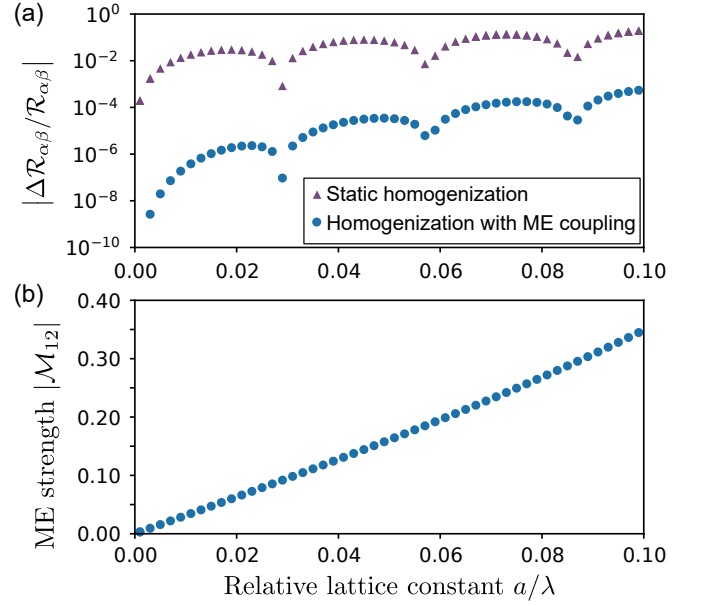


FIG. 3: Relative errors and effective ME coupling strengths versus normalized lattice constant  $a/\lambda$ , with all other parameters the same as in Fig. 2. (a) Relative error in  $\mathcal{R}_{\alpha\beta}$ , calculated using the static and ME homogenization schemes and compared to the transfer matrix results. Note the logarithmic scale on the vertical axis. (b) Magnitude of the off-diagonal element in the effective  $M$  matrix, which describes the strength of the ME coupling.

Once the angle of incidence reaches the critical value, the wave in the  $b$  layer becomes evanescent, but the wave in the  $a$  layer is propagating. Near  $\theta_{\text{crit}}$ , the reflection and transmission coefficients are found to depend strongly on the choice of layer order ( $\alpha\beta\dots$  or  $\beta\alpha\dots$ ), and both are very different from the value predicted by the static permittivity  $\epsilon_{\text{stat}}$ ; see [3] and Fig. 2.

For this setup, the fine-scale basis in our homogenization procedure contains Bloch waves with the tangential components of the Bloch wave vector  $q_{\tau m} = mn_{\text{stat}}k_0/(n_q - 1)$ , where  $0 \leq m < n_q$ . Only non-negative values of  $q_\tau$  are needed due to the symmetry of the structure in the tangential direction. For each  $q_\tau$  there are two Bloch waves in the forward and backward directions; hence the total size of the Bloch basis is  $2n_q$ . On the coarse level, the basis consists of the respective  $2n_q$  generalized plane waves. We will take  $n_q = 7$ ; the results shown below are essentially unchanged for other choices of  $n_q \geq 5$ .

Figure 2 plots the reflectance, and the phase of the reflection coefficient against the number of lattice periods  $N$  in the slab. (Each until cell has two layers, so the total number of layers is  $2N$ .) For all quantities, the results of the homogenization scheme agrees extremely well with the exact results obtained by transfer matrix calculations. As an example, Fig. 3(a) shows that the relative error in the reflection coefficient  $\mathcal{R}_{\alpha\beta}$  is at least two orders of magnitude lower than in the static approx-

imation. Notably, the homogenization captures the substantial differences between the  $\alpha\beta\dots$  and  $\beta\alpha\dots$  layer orderings [3] via the ME coupling in the  $\mathcal{M}$  tensor. For instance,

$$M(a/\lambda = 0.04) \approx \begin{bmatrix} 3.02 & 0 & 0.128i \\ 0 & 1 & 0 \\ 0.128i & 0 & 1 \end{bmatrix}. \quad (16)$$

The effective permittivity differs slightly from its static value of 3, but the key feature is the presence of the ME coupling terms, which are clearly appreciable. The magnitude of the ME coupling is approximately proportional to  $a/\lambda$  and vanishes in the static limit  $a/\lambda \rightarrow 0$ , as shown in Fig. 3(b).

In conclusion, we have demonstrated that a *local* homogenization procedure, which produces an effective ma-

terial tensor with magnetoelectric coupling terms, can accurately describe the behavior of periodic multilayer heterostructures away from the static limit. Specifically, the local homogenization correctly accounts for the effects of intrinsic and extrinsic symmetry breaking, one manifestation of which is a dependence of the reflection and transmission characteristics on the order of the layers, as noted in previous studies [3, 8].

The research of IT and ANMSH was supported in part by the US National Science Foundation awards DMS-1216970 and DMS-1620112. CYD was supported by the Singapore MOE Academic Research Fund Tier 3 Grant MOE2016-T3-1-006.

- 
- [1] A. V. Chebykin, A. A. Orlov, C. R. Simovski, Y. S. Kivshar, and P. A. Belov, *Phys. Rev. B* **86**, 115420 (2012).
  - [2] Y. Liu, S. Guenneau, and B. Gralak, *Proc. R. Soc. A* **469**, 2013.0240 (2013).
  - [3] H. Herzig Sheinfux, I. Kaminer, Y. Plotnik, G. Bartal, and M. Segev, *Phys. Rev. Lett.* **113**, 243901 (2014).
  - [4] A. Andryieuski, A. V. Lavrinenko, and S. V. Zhukovsky, *Nanotechnology* **26**, 184001 (2015).
  - [5] S. V. Zhukovsky, A. Andryieuski, O. Takayama, E. Shkondin, R. Malureanu, F. Jensen, and A. V. Lavrinenko, *Phys. Rev. Lett.* **115**, 177402 (2015).
  - [6] V. Popov, A. V. Lavrinenko, and A. Novitsky, *Phys. Rev. B* **94**, 085428 (2016).
  - [7] P. Yeh, *Optical Waves in Layered Media* (Hoboken, N.J.: John Wiley, 2005), ISBN 0471731927.
  - [8] X. Lei, L. Mao, Y. Lu, and P. Wang, *Phys. Rev. B* **96**, 035439 (2017).
  - [9] K. Mnasri, A. Khrabustovskyi, C. Stohrer, M. Plum, and C. Rockstuhl, *Physical Review B* **97**, 075439 (2018).
  - [10] R. J. Potton, *Reports on Progress in Physics* **67**, 717 (2004).
  - [11] C. F. Bohren, *Chemical Physics Letters* **29**, 458 (1974).
  - [12] S. Bassiri, C. H. Papas, and N. Engheta, *J. Opt. Soc. Am. A* **5**, 1450 (1988).
  - [13] N. Engheta and D. L. Jaggard, *IEEE Antennas and Propagation Society Newsletter* **30**, 6 (1988).
  - [14] I. Tsukerman and V. A. Markel, *Proc Royal Society A* **470**, 2014.0245 (2014).
  - [15] I. Tsukerman, *Physics Letters A* **381**, 1635 (2017).